

# Parametric interaction and intensification of nonlinear Kelvin waves

Vadim Novotryasov and Dmitriy Stepanov

V.I.Ilichev Pacific Oceanological Institute, Vladivostok, Russia

Observational evidence is presented for nonlinear interaction between mesoscale internal Kelvin waves at the tidal  $-\omega_t$  or the inertial  $-\omega_i$  frequency and oscillations of synoptic  $-\Omega$  frequency of the background coastal current of Japan/East Sea. Enhanced coastal currents at the sum  $-\omega_+$  and dif  $-\omega_-$  frequencies:  $\omega_{\pm} = \omega_{t,i} \pm \Omega$  have properties of propagating Kelvin waves suggesting permanent energy exchange from the synoptic band to the mesoscale  $\omega_{\pm}$  band. The interaction may be responsible for the greater than predicted intensification, steepen and break of boundary trapped and equatorially trapped Kelvin waves, which can affect El Niño. The problem on the parametric interaction of the nonlinear Kelvin wave at the frequency  $\omega$  and the low-frequency narrow-band nose with representative frequency  $\Omega \ll \omega$  is investigated with the theory of nonlinear weak dispersion waves.

## 1. Introduction

Internal Kelvin waves play a significant role in the dynamics of the oceans. There are two basic types of the waves: equatorially trapped and boundary trapped. Kelvin waves propagating on the equatorial thermocline participate in the adjustment of the tropical ocean to wind stress forcing [Philander, 1990]. Extensive data on Kelvin waves have been obtained recently, motivated in part by possible connection between the initial stages of El Niño and equatorial nonlinear Kelvin waves which may precede this event. Any relaxation or reversal of the steady trade winds (the easterlies) results in the excitation of a Kelvin wave, which can affect El Niño. In other words Kelvin waves play a critical role in generating and sustaining of the Southern Oscillation [e.g., Fedorov, 2000].

In the dynamics of the coastal oceans Kelvin waves are used to interpret such phenomena as the instability of along-shore currents, the generation and variability of wind currents on the shelf, and upwelling [Brink, 1991]. Fedorov and Melville [1995, 1996] considered Kelvin waves trapped boundaries and showed that waves could manifest nonlinear properties that is steepen and overturn or break. A wave of depression deepens the thermocline and breaks on the forward face of the wave. A broken wave of depression can form a jump [also called shocks or fronts: Lighthill, 1978; Philander, 1990]. In turn, the breaking of Kelvin waves may be important in mixing, momentum and energy transfer in coastal oceans. Other example of nonlinear Kelvin wave dynamics includes the problem of nonlinear geostrophic adjustment in the presence of a boundary [Helfrich et al., 1999; Reznik and Grimshaw, 2002].

The spectrum represents one of the major characteristics of the waves. It is used as a representative statistical description of the wave field in studies of nonlinear interaction [e.g., Hibiya et al., 1998], acoustic propagation [e.g., Colosi et al., 1998], and mixing parametrization [Polzin, 1995]. Filonov and Novotryasov [2005, 2007] studied the wave band of temperature fluctuation spectra in the coastal zone of Pacific Ocean and observed that in the high-frequency band of temperature spectra the spectral exponent tends to  $\sim \omega^{-1}$  at the time of spring tide and on the western shelf of the Japan/East Sea, in the  $\omega_i \ll \omega \ll N_*$  range, where  $N_*$  is the representative buoyancy frequency and  $\omega_i$  is the inertial frequency, the spectral exponent tends to  $\sim \omega^{-3}$ . These features Filonov and Novotryasov [2007] simulated by the model spectrum of nonlinear internal waves in the shallow water. They considered interaction of high-frequency waves with the wave at the tidal frequency and shown that the spectrum of high-frequency internal waves take the universal form and the spectral exponent tends to  $\sim \omega^{-1}$ .

In this paper, we present observational evidence for nonlinear interaction between synoptic oscillations of the background current at the representative frequency  $\Omega$  and nonlinear Kelvin waves at the tidal  $-\omega_t$  or the inertial  $-\omega_i$  frequencies. Findings are based on a well defined spectral peaks at the sum  $-\omega_+$  and dif  $-\omega_-$  frequencies of inertial, semidiurnal and synoptic motions measured by current meters and temperature records collected in the coastal Japan/East Sea. We made rotary spectral analyses of these records and found that the clockwise rotary spectrum for coastal currents measured at 35-m depth in the 1999 year has well-defined spectral peaks at the frequencies  $\omega_t \sim 1/12.4$ (cph),  $\Omega_{1,2} \sim 1/64, 1/102$ (cph), as well as sym and difference frequencies  $\omega_{\pm} = \omega_s \pm \Omega_{1,2}$  and their overtones  $\omega_n = n\omega_{\pm}$  ( $n = 1, 2, 3$ ). Analyses of coastal temperature records collected in the 2004 year showed that the spectrum of temperature variations has an analog form with spectral peaks at the inertial frequency  $\omega_i \sim 1/17.8$  (cph) and  $\Omega_{1,2} \sim 1/80, 1/160$  (cph) synoptic frequencies, as well as sym and difference frequencies  $\omega_{\pm} = \omega_i \pm \Omega_{1,2}$  and overtones  $\omega_n = n\omega_{\pm}$  ( $n = 1, 2, 3$ ).

With the theory of nonlinear interaction among weak dispersion waves [Gurbarov et al., 1990] we consider the problem on the parametric interaction of the nonlinear Kelvin wave at the frequency  $\omega$  and the low-frequency narrow-band nose with representative frequency  $\Omega \ll \omega$ . We show that nonlinear interaction between Kelvin wave and no stationary low-frequency component of the background coastal current excited by the atmospheric forcing leading to the intensification of tidal and inertial currents on the sub-surfers and near-bottom layers of the coastal zone. Analogy phenomena of the Kelvin wave intensification can occur in the equatorial ocean.

## 2. Observations

In the first experiment, observations of internal waves were performed at the coast of the Gamov Peninsula area

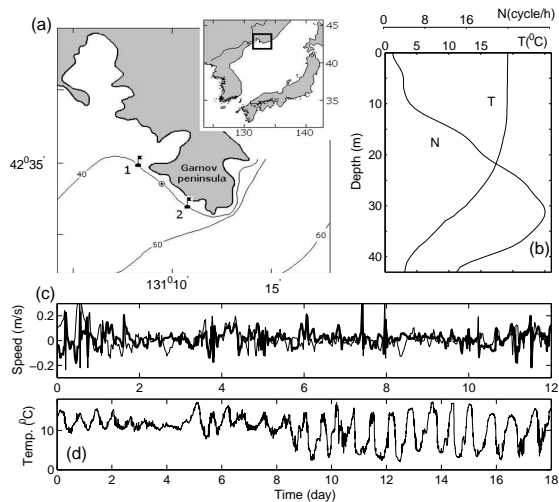


**Figure 1.** (a) Study area on the Japan/East Sea shelf, September 1999, 2004. The mooring location in 2004 is shown in Arabic. The circle indicates the mooring location in 1999 and the location of the mooring vessel, from which hourly casts were conducted on September, 1999, 2004. (b) Daily mean vertical profiles of temperature  $T$  and buoyancy frequency  $N$ . (c) Records of the meridional (light curve) and zonal (heavy curve) components of the current at the 35-m depth in autumn 1999. (d) Record of the temperature variations at the mooring buoy 1 in autumn 2004.

of the Japan/East Sea in 1999 year. The records of current meter collected from a mooring deployed water depth 40 m, during 2 weeks in September (Figure 1a). To gauge temperature, speed and direction of currents, the buoy was instrumented with the Russian-made POTOK integral instrument at a depth of 35 meters. The POTOK had a temperature measurement resolution of  $0.05^\circ\text{C}$ . The sampling rate was 15 minutes. The time series of the meridional (light curve) and zonal (heavy curve) current components from this mooring are shown on Figure 1c. The Canadian Guideline CTD profiler was used for the vertical profiling of water. The hydrostatic pressure, temperature and electric conductivity of seawater were measured during profiling. The profiling errors were no greater than  $0.01^\circ\text{C}$  in temperature and 0.02 psu in salinity. Figure 1b shows the mean temperature and buoyancy frequency profiles for the study site. Details of this experiment (results, methods of their processing, etc.) were reported by *Novotryasov, et. al* [2003].

In the second experiment, measurements of internal wave band temperature fluctuations were performed during 18 days starting 3 September 2004. The time records of temperature were collected from two moorings deployed along the coastline at a distance of 800m from it, approximately at 40m depth and separated by a distance of 5.5 km from each other. The first of them was deployed at 28m depth and the second one, at 35m depth (below the surface). The moorings were equipped with digital thermographs made by the Russian manufacturer. The devices had a measuring precision of  $0.05^\circ\text{C}$  for temperature. The sampling rate was 1 minutes. The temperature and salinity vertical profiles were performed on 20–21 September, from a vessel anchored between the moorings with the Canadian Guideline CTD profiler. In total, 25 hourly casts were made.

The obtained data were analyzed by unified standard spectral techniques [*Emery and Thomson, 1997*]. The approach involved (i) the elimination of low-frequency components with a Tukey’s cosine filter, (ii) the splitting of the resulting series into nine 37.2-hour segments (three semidiurnal tidal periods each), (iii) the calculation and averaging of spectral densities by segments, and (iv) the smoothing of the averaged spectral densities by a five-point Tukey’s filter. The number of degrees of freedom in the processing amounted to approximately 10 for the first experiment and 20 for the second, providing a reasonable reliability of the results of spectral analysis.

### 3. The model

A spectrum model of nonlinear interactions among internal Kelvin waves is developed. It is assumed that  $H/\lambda \ll 1$ , and  $A/H \ll 1$ , where  $H$  is the water depth,  $\lambda$  is a characteristic wave-length,  $A$  is a representative wave amplitude. The basic component of this model is the simple wave equation. For the first most powerful mode of the small-amplitude Kelvin waves the equation is written as

$$\partial u / \partial x - \alpha u \partial u / \partial \tau = 0, \quad (1)$$

where  $u(t, x)$  is the alongshore current,  $x$  is a horizontal coordinate,  $\tau = t - x/c$ ,  $t$  is time. The parameters  $\alpha$  and  $c$  are the coefficient of nonlinearity and the phase speed of long internal waves, respectively. Parameter of nonlinearity is determined by the background density and is related in the Boussinesq approximation as:

$$\alpha = \left( 3H \int_{-H}^0 \phi_z^3 dz \right) \times \left( 2c^2 \int_{-H}^0 \phi_z^2 dz \right)^{-1}, \quad (2)$$

where  $z$  is a vertical coordinate, positive upward. The phase speed  $c$  and the amplitude function of the wave mode  $\phi(z)$  are determined from the solution of the eigenvalue problem

$$d^2 \phi / dz^2 + c^{-2} N^2(z) \phi = 0, \quad (3)$$

with boundary condition

$$\phi(-H) = \phi(0) = 0, \quad (4)$$

and with the normalization

$$\phi_{\max} = 1. \quad (5)$$

Equation (1) is a basic model for study of Kelvin waves interaction. Let us consider interaction nonlinear Kelvin wave with frequency  $\omega_0$  (tidal  $\omega_t$  and inertial  $\omega_i$ ) and narrow-band synoptic noise (later SN) with frequency  $\Omega \ll \omega_0$  using the spectrum model of nonlinear internal waves described in terms of the equation (1). Let the alongshore current  $u(x, t)$  at the boundary of the coastal area  $x = 0$  be the superposition of internal wave with frequency  $\omega_0$ , amplitude  $A_0$  and the noise  $\vartheta(t)$  with typical frequency  $\gamma \ll \omega_0$

$$u(t, x = 0) = u_0(t) = A_0 \cos(\omega_0 t + \varphi) + \vartheta(t), \quad (6)$$

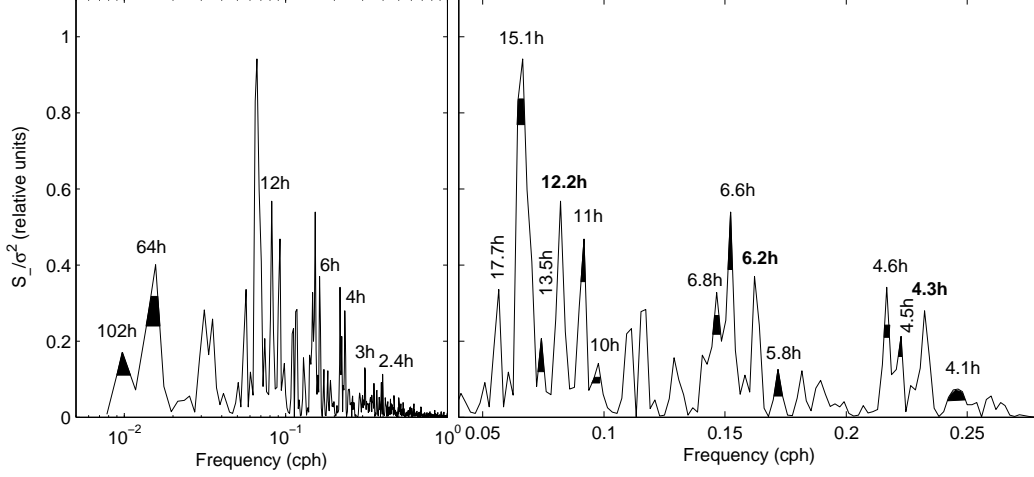


**Figure 2.** (a) Normalized clockwise rotary spectra of currents versus for current measured at 35-m depth in autumn 2004 near the Gamov peninsula. The numerical digits over peaks are their periods (h). (b) The increased fragment of the spectrum in the surrounding of the semidiurnal frequency. Dark numerals **12.2**; **6.2**; **4.3** are carrier periods (h).

where  $\varphi$  – is a random phase with uniform distribution in the interval  $[-\pi, +\pi]$ .

We confine our analysis to the wave evolution stage, which is characterized by condition  $x < x_*$ , where  $x_* = (\alpha A_0 \omega_0)^{-1}$ . In this stage the front Kelvin wave appears and it is not accompanied by generation of internal solitons. We introduce parameter  $d = x/x_*$ , which determine the similarity between a Kelvin shock-wave and the wave and consider the case  $d < 1$ . For this case the spectral density of the wave field  $u$  is

$$a(\omega; x) = -\frac{J_0(\omega d/\omega_0)}{2\pi i \omega \alpha x} \int_{-\infty}^{+\infty} \{\exp[-i\omega \alpha x \vartheta(t)] - 1\} e^{i\omega t} dt - \sum_{\substack{n=-\infty \\ n \neq 0}}^{\infty} \frac{i^n J_n(\omega d/\omega_0)}{2\pi i \omega \alpha x} \int_{-\infty}^{+\infty} \{\exp[in\varphi - i\omega \alpha x \vartheta(t)] - 1\} \times \exp[i(\omega - n\omega_0)t] dt \quad (7)$$

From equation (7) we can affirm that the first term is the spectral density of the synoptic oscillations and the second term is the spectral density of the Kelvin waves distorted by the synoptic oscillations.

We consider the spectral composition of the Kelvin wave near of the harmonics with the number  $n$  of the carrier frequency  $\omega_0$ . Given that  $\gamma \ll \omega_0$  we make replacement  $\omega$  at  $n\omega_0$  in the exponential rate of the equation (7). Then we obtain the equation for the harmonic with number  $n$

$$u_n(t, x) = A_n(x) \cos[n\omega_0 t + n(\varphi(t) - \omega_0 \beta x \vartheta(t))] \quad (8)$$

and her amplitude depending on the parameter  $d = A_0 \alpha \omega_0 x$  is

$$A_n(x) = 2J_n(nd)A_0/nd. \quad (9)$$

From the equation (9), we can affirm that the amplitude of the harmonic is decreased with increasing of harmonic number  $\sim 1/n$ .

Perform the more detailed spectral analysis of the nonlinear Kelvin waves, when the synoptic noise consists of regular

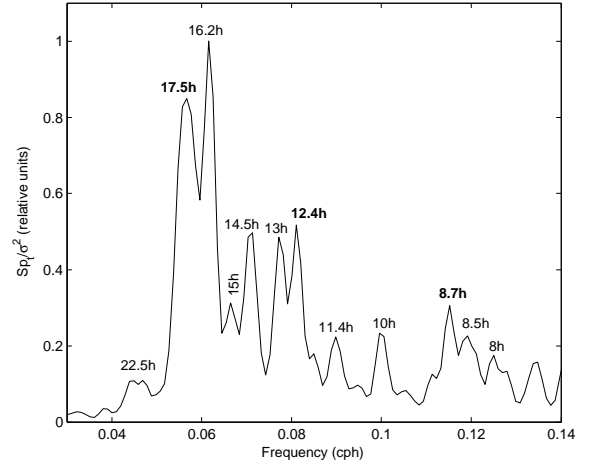


**Figure 3.** Normalized spectrum versus for record of the temperature variations at the mooring buoy 1 in autumn 2004 near the Gamov peninsula. The numerical digits over peaks are their periods (h).

and stochastic components:  $\vartheta(t) = a \cos(\Omega t) + \vartheta_{ns}(t)$ . Let the amplitude of the phase modulation related with regular component  $M = \alpha n \Omega x$  is small, that is  $M \ll 1$ . Let the Kelvin waves have narrow-band spectrum, and the synoptic noise width  $\gamma \ll \omega_0$ , besides the noise, amplitude and phase of Kelvin waves have Gaussian distribution. In this case the correlation function of the harmonic with number  $n$  taking into account the equation (8) is

$$B_n(\tau, x) = \left\{ \frac{A_n^2}{2} \left\{ \cos n\omega_0 \tau + \frac{(a\alpha n \omega_0 x)^2}{2} [\cos(n\omega_0 + \Omega)\tau] + \cos(n\omega_0 - \Omega)\tau \right\} \right\} \exp[-n^2 D_\psi \tau / 2], \quad (10)$$

where  $D_\psi(\tau) = D_\varphi(\tau) + (\alpha \omega_0 x)^2 (\sigma_{ns}^2 - B_{ns}(\tau))$ . Here  $D_\phi$  is the structure function of the Kelvin wave phase,

**Table 1.** The periods of the peaks of the temperature variations spectrum (digit numerals) and the calculated periods (light numerals)

$1/\Omega(h)$	$1/\omega_+(h)$	$1/\omega_s(h)$	$1/\omega_-(h)$	$1/\omega_+(h)$	$1/\omega_i(h)$	$1/\omega_-(h)$	$1/\omega_+(h)$	$2/\omega_i(h)$	$1/\omega_-(h)$
84	10.8	12.4	14.5	14.7	17.8	22.6	8.0	8.9	10.0
<b>84</b>	<b>11.0</b>	<b>12.4</b>	<b>14.5</b>	<b>15.0</b>	<b>17.5</b>	<b>22.5</b>	<b>8.0</b>	<b>8.7</b>	<b>10.0</b>
168	11.5	12.4	13.4	16.1	17.8	19.9	8.5	8.9	9.4
<b>168</b>	<b>11.5</b>	<b>12.4</b>	<b>13.0</b>	<b>16.2</b>	<b>17.5</b>	–	<b>8.5</b>	<b>8.7</b>	<b>9.5</b>

$B_{ns}(\tau) = \langle \vartheta_{ns}(t + \tau)\vartheta_{ns}(t) \rangle$  is the correlation function of the synoptic noise. We perform the Fourier transform of the correlation function  $B_n(\tau, x)$  and obtain the formula for the spectrum of the harmonic

$$S_n(\omega; x) = \frac{A_n^2}{2} \tilde{S}_n(\omega - n\omega_0) + \frac{(A_n a \alpha n \omega_0 x)^2}{4} \times \{ \tilde{S}_n(\omega - (n\omega_0 + \Omega)) + \tilde{S}_n(\omega - (n\omega_0 - \Omega)) \}, \quad (11)$$

where

$$\tilde{S}_n(\omega; x) = \frac{1}{2\pi} \int_{-\infty}^{+\infty} \exp[-n^2 D_\psi(\tau)/2] \cos(\omega\tau) d\tau. \quad (12)$$

From equation (10), we can affirm that spectrum of the wave have harmonics with frequencies  $n\omega_0$  as well as harmonics with sum and dif frequencies  $\omega_\pm = n\omega_0 \pm \Omega$  and amplitudes increasing with growth of distance traversed by the wave. This means that at the coastal zone between Kelvin waves and synoptic noise takes place nonlinear interaction, which is accompanied by intensification Kelvin waves with side frequencies  $\omega_\pm = n\omega_0 \pm \Omega$ .

#### 4. Discussion and Conclusion

Let us turn to the records of the current velocity. Figure 1c presents records smoothed by Tukey window with the width 1 h of the meridional (light curve) and zonal (heavy curve) components of the current in the coastal zone of Japan/East Sea in autumn 1999 year. It is of interest to note a low-frequency component of the variation in the record of the current velocity. Let us analyze circular rotary current component with the rotary spectral analysis [Emery and Thomson, 1997]. The spectrum of the clockwise rotary (CWR) component of the velocity is

$$S_-(\omega) = 0,125 \cdot (S_{uu} + S_{vv} - 2Q_{uv}),$$

where  $S_{uu}$  and  $S_{vv}$  are the one-sided autospectra of the  $u$  and  $v$  Cartesian components of the velocity and  $Q_{uv}$  is the quadrature spectrum between the two components. These spectra were determined by unified statistical spectral techniques using the algorithms presented in [Emery and Thomson, 1997]. The spectra have  $N$  degrees of freedom, where  $N \geq 10$ . Figure 2a shows the CWR spectrum of currents versus  $\log \omega$  normalized by maximal value. It is of interest to note the groups of the well defined significant spectral peaks in the surrounding of the semidiurnal frequency and

her 1, 2, 3 and 4 harmonics. Our estimations show that the magnitudes of these spectral peaks interrelated with number harmonics by the approximate relation

$$A_{12} : A_6 : A_4 : A_3 : A_{2,4} \approx 1 : 2 : 3 : 4 : 5$$

(with error  $< 20\%$ ).

There are two peaks with light and heavy tops at the representative frequencies  $\Omega_1 \sim 1/64$  and  $\Omega_2 \sim 1/102$  (cph) in the low-frequency band of the spectra.

Figure 2b presents the increased fragment of the spectrum in the surrounding of the semidiurnal frequency. It is of interest to note a significant well defined spectral peak at the  $\omega_s = 1/12.2$  (cph) frequency surrounded by side peaks with dark end light tops. Not hard to make sure that the frequencies of these picks are determined by formula  $\omega_\pm = \omega_s \pm \Omega_{1,2}$  with error equals of experimental error uncertainty. In particularly the strong spectral peak at the difference frequency  $\omega_- = 1/12.2 - 1/64$  (cph) suggests that the motion in study region is dominated by not only the tide movements, but and the inertial movements. The pick at the frequency  $\omega_i = 1/17.7$  (cph) is formed by the inertial movements. Thus the spectrum has fine structure in the band 1/14 - 1/16.5 (cph), which don't segregate with help our dates and methods of analyses.

Let us consider the structure of the spectrum in surroundings of the harmonics of semidiurnal frequency  $\omega_s$  (Figure 2b). As in the past picks at the carrier frequencies:  $\omega_{s1}, \omega_{s2}$  are surrounded by side picks at the frequencies, which are determined by formula  $\omega_\pm = \omega_{s1,2} \pm \Omega_{1,2}$ .

Thus spectral analysis of the clockwise rotary velocity shows that her spectrum is determined by oscillations with the tidal frequency  $\omega_s \approx 1/12.2$  (cph) and the frequencies  $\Omega_{1,2} \approx 1/72, 106$  (cph) from synoptic band and also that spectrum has the fine structure in the neighborhood of the frequency  $\omega_s$  with side peaks at the frequencies, which are determined by formula  $\omega_\pm = \omega_s \pm \Omega_{1,2}$ . The similar structure has spectrum in the neighborhood of the first and the second harmonics of the semidiurnal frequency  $\omega_s$ .

Then turn to the records of the temperature of the coastal water of Japan/East sea collected in autumn 2004 year. Figure 3 shows the averaged spectrum of the temperature records collected from two moorings and normalized by the maximum value of the spectrum. Spectra are calculated by unified standard spectral techniques [Emery and Thomson, 1997]. The number of freedom degrees amounted to approximately 20.

Of particular interest are the groups of the significant spectral peaks at the inertial frequency and her first harmonic and also the peaks in the surrounding of the semidiurnal frequency  $\omega_s$ .

Arabic numerals over spectral peaks equal the periods (hour) of these peaks. These periods (h) are placed in the Table 1. Digit numerals equal the periods of the spectral peaks and light numerals equal the periods calculated by the formula  $1/\omega_{\pm} = 1/\omega_{s,i} \pm 1/\Omega_{1,2}$ .

As indicated by Table 1 the periods of the spectral peaks and the periods calculated by the formula have approximately equal values. Thus the spectral analysis of current and temperature meter records of the Japan/East Sea coastal water shows that the spectrum is determined by oscillations with frequencies of near inertial  $\omega_i \approx 1/17.8$  (cph) and tidal  $\omega_s \approx 1/12.2$  (cph) frequencies as well as the frequencies  $\Omega_{1,2} \approx 1/72, 106$  (cph) from synoptic band. The analysis shows that the spectrum has the fine structure in the neighborhood of the frequencies  $\omega_{i,s}$  with side picks at the frequencies, which are determined by formula  $\omega_{\pm} = \omega_{i,s} \pm \Omega_{1,2}$ . The similar structure has spectrum in the neighborhood of the first harmonics of the inertial frequency  $\omega_i$ .

As a conclusion, we showed that among nonlinear internal Kelvin wave with frequency  $\omega$  and the low-frequency narrow-band nose with representative frequency  $\Omega \ll \omega$  occur the parametric interaction, i.e. among the low-frequency band and high-frequency band of internal Kelvin waves occur the energy exchange. Hence, as a result of nonlinear interaction the energy of internal Kelvin waves in the coastal and tropical oceans can grow at the expense of the low-frequency narrow-band nose energy.

#### Acknowledgments.

This work was supported by the Presidential Grant No. MK-1364.2008.5 by the Prezidium of the Russian Academy of Sciences (Program "Mathematical methods in nonlinear dynamics." Project No. 06-I-13-048).

## References

- Emery, W. J., and R. E. Thomson (1997), *Data Analysis Methods in Physical Oceanography*, 634 pp., Pergamon, New York.
- Brink, K. H. (1991), Coastal-trapped waves and wind-driven currents over the continental shelf *Ann. Rev. Fluid Mech.*, *23*, 389–412.
- Colosi, J. A., and the ATOS Group (1999), A review of recent results on ocean acoustic wave propagation in random media: Basin scales, *IEEE J. Oceanic Eng.*, *24*, 138–155.
- Fedorov, A. V., and W. K. Melville (1995), Propagation and breaking of nonlinear Kelvin waves, *J. Phys. Oceanogr.*, *25*, 2518–31.
- Fedorov, A. V., W. K. Melville (1996), Hydraulic jumps at boundaries in rotating fluids, *J. Fluid Mech.*, *324*, 55–82.
- Fedorov, A. V., W. K. Melville (2000), Kelvin fronts on the equatorial thermocline, *J. Phys. Oceanogr.*, *30*, 1692–705.
- Filonov, A., and V. Novotryasov (2005), Features of the nonlinear wave spectrum in the coastal zone, *Geophys. Res. Lett.*, *32*, L15602, doi: 10.1029/2005GL023046.
- Filonov, A., and V. Novotryasov (2007), On a spectrum of nonlinear internal waves in the oceanic coastal zone, *Nonlin. Processes Geophys.*, *14*, 757–762.
- Gurbatov, S.N., A.N. Malakhov, and A.I. Saichev (1990), *Nonlinear Random Waves in Media with Zero Dispersion*, 215 pp., Nauka, Moscow.
- Helfrich, K.R., A.C. Kuo, L.J. Pratt (1999), Nonlinear Rossby adjustment in a channel, *J. Fluid Mech.*, *390*, 187–222.
- Hibiya, T., Y. Niwa and K. Fujiwara (1998), Numerical experiments of nonlinear energy transfer within the oceanic internal wave spectrum, *J. Geophys. Res.*, *103*, 18715–17722.
- Lighthill, M. J. (1978), *Waves in Fluids*, 504 pp., Cambridge University Press, UK.
- Novotryasov, V. V., N. S. Vanin, A. A. Karnaukhov (2005), Manifestation of nonlinear properties of Kelvin internal waves in the coastal zone of the sea of Japan, *Izv. Atm. and Ocean. Phys.ics.*, *41*, 611–619.
- Philander S.G. (1990), *El Niño, La Niña and the Southern Oscillation*, 293 pp., Academic Press, New York.
- Polzin, K. L., J. M. Toole and R. W. Schmitt (1995), Finescale parametrization of turbulent dissipation, *J. Phys. Oceanogr.*, *25*, 306–328.
- Reznik, G.M. and R. Grimshaw (2002), Nonlinear geostrophic adjustment in the presence of a boundary, *J. Fluid Mechanics*, *471*, 257–283.
- Vadim Novotryasov, V.I.II'ichev Pacific Oceanological Institute of the Russian Academy of Sciences, 43 Baltiiskaya Street, 690041 Vladivostok, Russia. (vadimnov@poi.dvo.ru)
- Dmitriy Stepanov, V.I.II'ichev Pacific Oceanological Institute of the Russian Academy of Sciences, 43 Baltiiskaya Street, 690041 Vladivostok, Russia. (step-nov@poi.dvo.ru)